Applied Catalysis A: General 487 (2014) 1–15

Contents lists available at ScienceDirect

Applied Catalysis A: General

journal homepage: www.elsevier.com/locate/apcata

Hydrogenation of cinnamaldehyde in the presence of PdAu/C catalysts prepared by the reverse "water-in-oil" microemulsion method

T. Szumełda, A. Drelinkiewicz*, R. Kosydar, J. Gurgul

Institute of Catalysis and Surface Chemistry, Niezapominajek 8, 30-239 Kraków, Poland

ARTICLE INFO

Article history:
Received 5 June 2014
Received in revised form 27 August 2014
Accepted 28 August 2014
Available online 6 September 2014

Keywords:
Pd–Au
Bimetallic
Cinnamaldehyde hydrogenation

ABSTRACT

Liquid phase hydrogenation of cinnamaldehyde was studied on carbon supported (Vulcan XC72) – PdAu catalysts with Au/Pd atomic ratio varying from 0.1 up to 2.1. Colloid-based method, namely the reverse "water-in-oil" microemulsion technique was used to prepare the catalysts. Accordingly, pre-formed metal nanoparticles of controlled size with a narrow size distribution were deposited on carbon support. The BET, XRD, XPS, SEM, TEM, and HRTEM techniques were employed to characterize PdAu/C catalysts and their monometallic 2%Pd/C and 2%Au/C counterparts. The metal particles were spherically shaped, nearly monodispersed and well distributed throughout the carbon support. The particles of low Au-content (Au/Pd < 0.8) were of smaller size than Pd (6.7 nm), and the particle size gradually increased approaching almost the size of Au (8.2 nm) at Au/Pd = 2.1. It was found that the content of Au influenced both activity and selectivity of PdAu/C catalysts for cinnamaldehyde hydrogenation. The C=C group of cinnamaldehyde was preferentially hydrogenated compared to the carbonyl (C=O) group on the Pd/C catalyst. At Au/Pd < 0.8 the effect of Au-content was relatively weak as reflected in the small decrease in the activity with only slight increase in the reactivity to C=O hydrogenation. The effect of Au manifested distinctly on Au-rich catalysts (Au/Pd > 1) giving strongly reduced activity to saturated aldehyde formation accompanied by the selectivity preference to the carbonyl group reduction. These activity/selectivity effects induced by the gold were discussed to be related with the microstructure of metal particles determining their surface composition. Moreover, both geometric and electronic modifications of Pd-sites due to the Pd–Au interactions should be also taken into account. These interactions may also provide new active sites which are able to activate the C=O bond of CAL in the PdAu alloy particles-containing catalysts.

1. Introduction

The utilization of bimetallic nanoparticles either in the form of colloids or supported catalysts has received enormous attention because they are very effective for the transformation of organic compounds to highly useful chemical products. Supported bimetallic catalysts are commonly prepared by conventional methods, such as co-impregnation and deposition-precipitation. These methods usually produce relatively large metal particles with a broad size distribution. Therefore, much attention has been paid to the colloid-based methods [1,2]. The advantage is that the colloidal particles are homogeneous in the composition and the size. Various methods have already been employed and co-reduction of metal ions precursors in the presence of the protective polymers, poly(vinylpyrrolidone) (PVP) or poly(vinyl alcohol) (PVA) was the most frequently used procedure. The first producing colloidal PdAu, PtAu, PdPt nanoparticles of true alloy structure [3–5] was also effectively adopted to synthesize SiO_2 and Al_2O_3 supported PdAu catalysts [6–8]. The use of method with PVA allowed to prepare PdAu/C and PdAu/TiO_2 catalysts with the particles of alloy structure with significantly narrower size distribution as compared to those obtained by the impregnation methods [2,9]. Recently, THPC (tetrakis(hydroxypropyl)phosphonium chloride), which acted as both a stabilizer and a reducing agent was applied to synthesize SiO_2, Al_2O_3, TiO_2 supported PdAu catalysts [2,10]. The reverse "water-in-oil" microemulsion (ME) is the other colloid-based synthesis method which has already been successfully applied for the preparation of various nanoparticles, including metals (Pt, Pd, Co, Ni, etc.), metal oxides (Al_2O_3, TiO_2, CeO_2 etc.), salts ($BaSO_4$, ZnS,), polymers [11–13] and supported monometallic Pd, Pt, Co catalysts [14–19].

The reverse "water-in-oil" microemulsion consists of nanosized water droplets surrounded by an organic phase and stabilized

* Corresponding author. Tel.: +48 126395114.
E-mail address: ncdrelin@cyf-kr.edu.pl (A. Drelinkiewicz).

http://dx.doi.org/10.1016/j.apcata.2014.08.036
0926-860X/

by a surfactant. These water droplets act as nanoreactors and provide size control for the formed nanoparticles. Thus, the treatment of water droplets containing metal ion precursor with reducing agent produces metal nanoparticles which are generally very fine with a narrow size distribution. In general, the particle size distribution in supported catalysts prepared by ME is significantly narrower as compared with those synthesized by commonly used impregnation methods. Using ME method it is also possible to achieve a good control of the particle size. The experimental parameters that determine the size of metal nanoparticles can be shortly summarized as the nature of surfactant, water to surfactant molar ratio (*W*), concentration and the type of metal precursor [$PdCl_2$, $Pd(NH_3)_4Cl_2$], and the type of reducing agent ($NaBH_4$, N_2H_4, H_2). In order to prepare supported catalyst, destabilization of microemulsion-containing pre-formed metal particles is carried out by slow addition of organic solvent (most frequently tetrahydrofurane THF) in the presence of carrier material. This stage plays an essential role in the dispersion/distribution of metal particles in final catalysts. The bulk oily phase in the combination with the hydrophobic character of the support surface determine the support – microemulsion interaction, and thus the distribution of metal particles in final catalysts [17,18]. Hydrophobic character of the support facilitates chemical compatibility between the microemulsion and the support surface favoring a better wetting of the support by organic bulk phase thus improving the dispersion/distribution of the metal particles.

The advantage of the microemulsion method is its potential for the preparation of bimetallic particles. Simultaneous reduction of both metal ion components accomplished in water pool offers the possibility to synthesize bimetallic particles of uniform size and well-defined compositions. The kinetics and mechanism of bimetallic colloidal PdPt, PtAu and PdAu particles formation by ME method are reported in series of papers by Wu et al. [20–22]. The composition of these bimetallic particles was roughly consistent with that of the precursor solutions and they had essentially a homogeneous alloy structure. However, their outer surface differed from the bulk. For instance, the outer surface of colloidal PdAu nanoparticles was Pd-rich [21].

Most publications devoted to bimetallic catalysts prepared by ME method concern electrocatalysts (PtRu, PtNi, PtCo, PtFe, PdAu, AuAg, PtAu) for the polymer membrane fuel cell, methanol oxidation and oxygen reduction reactions [23–25]. The suitability of the microemulsion method is also reflected by an increasing number of published works dealing with the supported bimetallic catalysts for various organic transformations such as PtIr/boehmite for the ring opening reaction in indan [26], $PdPt/Al_2O_3$ for hydrogenolysis and isomerization [27], NiB nanoparticles for hydrogenation of carbonyl and olefinic groups [28], $PtNi/Al_2O_3$ for 1,3-butadiene hydrogenation [29].

In the present work the reverse "water-in-oil" microemulsion method is utilized to prepare a series of carbon black (Vulcan XC72) supported PdAu catalysts with Au/Pd ratio ranging from 0.1 up to 2.1.

The modification of Pd-sites reactivity by Au is a well known phenomenon observed in a number of catalytic reactions, such as oxidation of alcohols [30] and glycerol [31], direct synthesis of hydrogen peroxide from H_2 and O_2 [9], hydrodesulfurization [6], and hydrodehalogenation [32]. The reactivity of PdAu catalysts in the hydrogenation reactions was definitively less extensively studied. Nevertheless, there are reports showing that the addition of Au has an impact on the reactivity of Pd in the hydrogenation of aromatic compounds [8], acetylene [33,34], butadiene [2,35], and 2-hexyne [36]. This effect has been also recently studied for the hydrogenation of cinnamaldehyde (CAL) and citral, the examples of α,β-unsaturated aldehydes. The hydrogenation of CAL can proceed either at C=C or C=O groups (Scheme 1) [37,38]. The former gives saturated aldehyde (hydrocinnamaldehyde, HCAL), the latter leads to unsaturated alcohol (cinnamalcohol, COL). These products have industrial (pharmaceutic, perfurmery) and biological applications. Recently, hydrocinnamaldehyde was found to be an important intermediate in the synthesis of pharmaceuticals used in the treatment of HIV. The hydrogenation of C=C bond in α,β-unsaturated aldehydes is thermodynamically favored thus making much more difficult the hydrogenation of the C=O bond yielding unsaturated alcohols. Yang et al. [39] reported that insertion of a small amount of Au leading to Au/Pd = 0.1–0.2 produced mesoporous supported alloy PdAu particles of smaller size than that of pure Pd but enhanced activity for cinnamaldehyde hydrogenation. This activity improvement was attributed to synergistic Pd–Au effect, which however had only slight impact on the selectivity control. High selectivity to C=C hydrogenation yielding saturated aldehyde typical for initial Pd catalyst (ca. 88%) only slightly increased (ca. 90%) on these PdAu catalysts with low Au contents [39]. Similar activity/selectivity effects were also observed for Al_2O_3, SiO_2 and C supported nanostructured Pt-on-Au catalysts [40,41] in which a small amount of fully dispersed Pt entities were deposited onto the surface of pre-formed colloidal Au particles. The Pt entities resulted in dramatic enhancement of Au activity without altering the selectivity of Au-catalyst. The high selectivity to C=C hydrogenation (70–80%) observed on Au/SiO_2 catalyst [42] was preserved on these nanostructured Pt-on-Au catalysts. In these catalysts the Pt entities were acting as the activity promoter of Au only, since the selectivity propensity of Au for the hydrogenation of CAL (and other carbonyl reactants) was not changed by

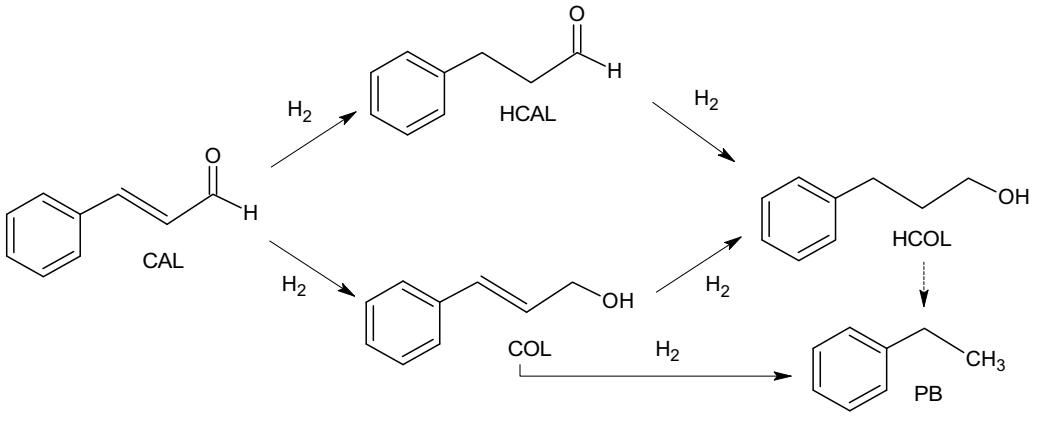

Scheme 1. Hydrogenation pathways of cinnamaldehyde.

the presence of Pt. The Pt sites were responsible for the activation of H_2 molecules while activation of aldehyde occurred on the Au sites and the activity improvement was due to H_2 spillover effect. The Pt entities activated hydrogen which migrated by spillover toward nearby Au sites on which aldehyde molecule is adsorbed. By hydrogen spillover effect also the enhanced activity of physically mixed less active Au/TiO_2 with Pd/TiO_2 catalysts in hydrogenation of citral was explained [43]. Simultaneously the selectivity to C=C hydrogenation was increased. Catalytic performance of ordered mesoporous carbon containing separate Au and Pd nanoparticles was also explained by hydrogen spill-over effect [44]. It resulted in promotion of C=C selectivity giving HCAL accompanied by much higher activity compared to monometallic Pd.

In the present work, the hydrogenation of cinnamaldehyde (CAL) has been chosen for exploring the catalytic performance of PdAu/C catalysts synthesized by the microemulsion method. The catalysts with fixed Pd loading (2 wt%) and the content of Au ranging from very small as in Au-poor (Au/Pd = 0.1) catalyst up to as high as Au/Pd = 2.1 in Au-rich catalysts are prepared. Their monometallic Pd and Au counterparts are also synthesized. Carbon black Vulcan XC72 is used as the support because of its advantageous textural characteristics, among them extended mesoporous structure and hydrophobous character [45]. Our intention is to exploit reactivity of these systems for CAL hydrogenation and in particular the capability of the Au-presence to control the C=C/C=O selectivity.

2. Experimental

2.1. Catalysts preparation

Carbon support Vulcan XC72 (supplied by CABOT) was used as the support. The catalysts consisting of the same palladium loading equal to 2 wt.% Pd and the growing Au content ranging from 0.4 wt% up to 6 wt% were prepared by means of reverse "water-in-oil" microemulsion method according to our previously published procedure [18,19]. In the PdAu/C catalysts the molar ratio of Pd:Au ranges from 1:0.1 up to 1:2.1 and they are designated PdAu-y, where y represents the Au/Pd molar ratio (the number of Au moles per 1 mol of Pd). The monometallic 2 wt% Pd/C and 2 wt% Au/C catalysts were also prepared using the same preparation procedure.

The reverse micellar solutions were prepared using polyoxyethylene(7-8)octylphenyl ether (Triton-X 114) (Aldrich) as the surfactant and cyclohexane (Aldrich) as the oil phase.

The aqueous solutions of $PdCl_2$ (molar ratio of $NaCl:PdCl_2 = 2$, Pd^{2+} ions concentration of 0.2 mol/dm^3 and $HAuCl_4$ (0.05 mol/dm^3) were used as the precursors, and hydrazine hydrate ($N_2H_4 \times H_2O$, N_2H_4 64–65%, reagent grade 98%, Aldrich) was used as reducing agent. Taking into account our previous studies [18] the value of parameter W equal to 5 was applied.

The solution of TRITON-X-114 in cyclohexane (surfactant concentration of 0.62 mol/dm^3) was prepared. In order to prepare 1 g of 2%Pd/C catalyst 0.94 cm^3 of $PdCl_2$ solution was added to 16.8 cm^3 cyclohexane-surfactant solution and the obtained suspension was vigorously stirred up to the formation of transparent, clear dark orange solution. In the preparation of PdAu catalysts a mixture of $PdCl_2$ and $HAuCl_4$ solutions of appropriate volume ratio and the cyclohexane solution of higher surfactant concentration giving the parameter $W = 5$ was prepared. The hydrazine (64–65%) was added directly to the microemulsion using the reducing agent to metal molar ratio of 20. The reduction of metal ions was quick, and the color of liquid quickly changed to black. Stirring was then continued for another 1 h. Then, carbon support (0.98 g) was introduced and the system was kept under stirring for 1 h. Deposition of metal nanoparticles on the support was carried out by introducing the THF solvent at a very slow rate 0.25 cm^3/min with the aid of the automatic syringe pump. The system was vigorously stirred. The volume of THF added was 3–4 times the volume of the microemulsion. Upon addition of THF, the color of liquid gradually changed from black to gray and finally the liquid was colorless, showing complete deposition of metal particles on the support. The obtained catalyst was separated by filtration, dried in air for ca. 24 h and washed with copious amount of methanol and acetone six times and filtrated in between. Finally, the catalysts were washed with water up to the removing of chloride ions, dried overnight in air and then at 120 °C for 16 h.

2.2. Methods of characterization

The X-ray diffraction (XRD) patterns were obtained with a Philips X'PERT diffractometer using Cu Kα radiation (40 kV, 30 mA). The average diameter of Pd particles was calculated on the basis of the Pd (1 1 1) peak broadening according to Scherrer equation (taking into account instrumental broadening).

The X-ray Photoelectron Spectroscopy (XPS) measurements were carried out with a hemispherical analyzer (SES R4000, Gammadata Scienta). The unmonochromatized Al Kα and Mg Kα X-ray source with the anode operating at 12 kV and 20 mA current emission was applied to generate core excitation. All binding energy values were corrected to the carbon C 1s excitation at 285.0 eV. The samples were pressed into indium foil and mounted on a holder. All spectra were collected at pass energy of 100 eV except survey scans which were collected at pass energy of 200 eV. Intensities were estimated by calculating the integral of each peak, after subtraction of the Shirley-type background, and fitting the experimental curve with a combination of Gaussian and Lorentzian lines of variable proportions (70:30).

Electron Microscopy (SEM, TEM) studies were performed by means of Field Emission Scanning Electron Microscope JEOL JSM–7500F equipped with the X-ray energy dispersive (*EDS*) system. Two detectors were used and the images were recorded in two modes. The secondary electron detector provided SEI images, and back scattered electron detector provided BSE (COMPO) micrographs. The catalyst sample was mixed with methanol and the obtained slurry was further treated with ultrasounds (5–10 min). Then, a droplet of the solution was put onto a grid, dried in air and used in the TEM instrument.

To prepare the particle size distribution diagram and estimation of the average particle size (d), at least 100 particles (N) were manually counted. The average metal particle diameter was calculated as the average of individual diameters from the formula:

$$d = \frac{\sum n_i d_i}{\sum n_i}$$

where n_i is the number of particles having diameter d_i

The counting was carried out on electron micrographs registered starting from 100 000 to 200 000 magnifications, where metal (Pd, Pd/Au, Au) particles contrasted very well with the support and they were clearly detected. On these micrographs registered in BSE (COMPO) mode the accuracy of the particle size scale was 0.5 nm.

HRTEM and STEM studies were performed on FEI Tecnai G^2 transmission electron microscope operating at 200 kV equipped with EDAX EDX and HAADF/STEM detectors. Samples for analysis were prepared by placing a drop of the suspension of sample in ethanol or THF onto a carbon-coated copper grid, followed by evaporating the solvent.

2.3. Hydrogenation reactions

Hydrogenation experiments were carried out in an agitated batch glass reactor at constant atmospheric pressure of hydrogen at temperature of 22 °C following the methodology previously described [46,47]. Toluene was used as the solvent.

In the initial stage of hydrogenation experiment, the catalyst and the solution were placed in the reactor in such a way that there was no immediate contact between them. The catalyst was activated "in situ" by passing nitrogen (20 min) and subsequently hydrogen (30 min) at temperature of 22 °C before the hydrogenation test. Then, the catalyst was contacted with the hydrogenated solution and the experiment started. The progress of the reaction was monitored by measuring the hydrogen consumed against reaction time. Samples of solutions were withdrawn from the reactor via a sampling tube at appropriate intervals of time and they were analyzed by GC.

Products analysis was performed with a gas chromatograph PE Clarus 500 equipped with a flame ionization detector under the following conditions: capillary column Elite-5 MS (30 m × 0.25 mm × 0.25 μm coating) with helium as a carrier gas (flow rate 1 ml/min) and injection temperature 250 °C. Product separation was obtained using temperature ramps: 65 °C for 1 min, 65–108 °C (15 °C/min), 108–115 (5 °C/min), 115–265 (15 °C/min) to 265 °C hold for 3 min. Decane (Sigma–Aldrich) was used as the standard.

Typically the hydrogenation test was carried out at 22 °C using 20 cm^3 of cinnamaldehyde solution in toluene of $c^0 = 0.05$ mol/dm^3 and catalyst concentration 5 g/dm^3. The same conditions were used in hydrogenation of HCAL as the substrate. In hydrogenation of cinnamalcohol (COL) reactant ($c^0 = 0.05$ mol/dm^3) the concentration of catalyst was lower and equal to 0.25 g/dm^3.

Shaking of the reactor was carried out at such a speed to ensure that the rate of hydrogen uptake did not depend on agitation speed. External diffusion resistance was ruled out, since no significant variation in the catalytic results was observed by increasing the agitation speed.

The conversion (C; %), selectivity to hydrocinnamaldehyde [S(HCAL); %], saturated alcohol [S(HCOL); %] and propyl benzene [S(PB); %] were calculated with the formulas

$$C_{CAL} = \frac{N_{CAL,0} - N_{CAL}}{N_{CAL,0}} \times 100\% \quad (1)$$

$$S_i = \frac{N_i}{N_{HCAL} + N_{HCOL} + N_{PB}} \times 100\% \quad (2)$$

where $N_{CAL,0}$ and N_{CAL} are the moles of CAL initially present in the reactor and the moles of CAL remaining at time t, respectively; N_{HCAL}, N_{HCOL} and N_{PB} are the numbers of moles of hydrocinnamaldehyde (HCAL), saturated alcohol (HCOL) and propyl benzene (PB) in the reaction mixture at the time t.

3. Results and discussion

3.1. Characterization of catalysts

All catalysts studied in this work were prepared using the same microemulsion composition with the same value of parameter $W = 5$. Textural properties of studied catalysts are collected in Table 1. As described before, carbon black Vulcan XC72 is used in the present studies because of its advantageous textural characteristics and hydrophobic surface. As shown in Table 1, the carbon material has surface area of 228 m^2/g and it exhibits an extended mesoporous structure evidenced by high contribution of mesopores (1.72 cm^3/g) relative to that of micropores (0.0484 cm^3/g). The pore size distribution diagram indicates the domination of pores of 1.7–2.5 nm in diameter (Supplementary Fig. S1). These textural features are consistent with the literature data [45,48,49]. Electron microscopic images (see below) indicate that the carbon material is composed of aggregated quasi spherical particles with a size within 20–50 nm. These carbon particles are constituted of groups of parallel graphene planes separated by about 0.35–0.5 nm, which are structured into little crystalline phases. They are observed as a very broad reflection centered at $2\theta = 43–44°$ in the XRD pattern of carbon material (Fig. 1).

Deposition of pre-formed metal particles results in distinct changes in textural characteristics of carbon support. The specific surface area is reduced and is accompanied by remarkable changes in the porous structure (Supplementary Fig. S1). As the content of Au, and thus the total metal content (Pd + Au) in the catalysts increases, the surface area decreases. Simultaneously, the volume of micropores decreases whereas that of mesopores does not essentially change (Table 1). Pore distribution profiles indicate that apart from some changes in the micro structure, distinct changes in a mesoporous structure appear also. As XRD and microscopic data show (see below) the metal particles in the PdAu/C catalysts are of 5–8 nm in size, e.g. they are too large to be introduced inside the micropores. Therefore, it may be assumed that the mesoporous structure of the carbon material allows metal particles to adsorb at the entrance of micropores with consequent blockage of micropores. Similar effect was observed during preparation of Vulcan XC72 supported electrocatalysts consisting of Pd–Pt nanoparticles [48] or after modification with organic dopants [49].

Table 1
Physicochemical characterization of the catalysts, Au/Pd atomic ratio determined by EDS and STEM, and the initial rate of cinnamaldehyde hydrogenation.

Sample	Surface area [m^2/g]	Porosity [cm^3/g]			Metal particle size d [nm]		Au/Pd atomic ratio		Initial rate R [mol CAL 10^{-5} min^{-1} g(cat)$^{-1}$]	TOF_{IN} *** [min^{-1}]
		Total	Meso	Micro	SEM	XRD	EDS	STEM		
Carbon	228	1.77	1.722	0.0484			–	–	–	–
Pd/C					6.7	5.5–6			22.7	1.21
PdAu-0.1 ($Pd_{91}Au_9$)*	204	1.41	1.37	0.0358	5.5	5.5	No data**	13/87	22.1	1.07
PdAu-0.2 ($Pd_{83}Au_{17}$)	188	1.42	1.39	0.0263	4.8				21.4	0.95
PdAu-0.4 ($Pd_{71}Au_{29}$)	179	1.40	1.38	0.0212	5.2	4–4.5	32/68		18.5	0.70
PdAu-0.8 ($Pd_{56}Au_{44}$)					5.3	5.5–6	55/44; 54/46		12.1	0.36
PdAu-1.8 ($Pd_{36}Au_{64}$)	166	1.34	1.32	0.0167	7.5	6.5–7	63/37; 65/35; 64/36	62/38; 70/30	7.8	0.15
PdAu-2.1 ($Pd_{32}Au_{68}$)	138	1.38	1.37	0.0066	7.8	7–7.5	69/31; 66/34	66/34; 62/38; 74/26	4.0	0.07
Au/C					8.2	8–9				–

* Nominal composition from the preparation.
** Not determined because of very weak signal.
*** Calculation of TOF_{IN} (min^{-1}) from initial hydrogenation rate. TOF numbers were calculated on the basis of total loading of metals.

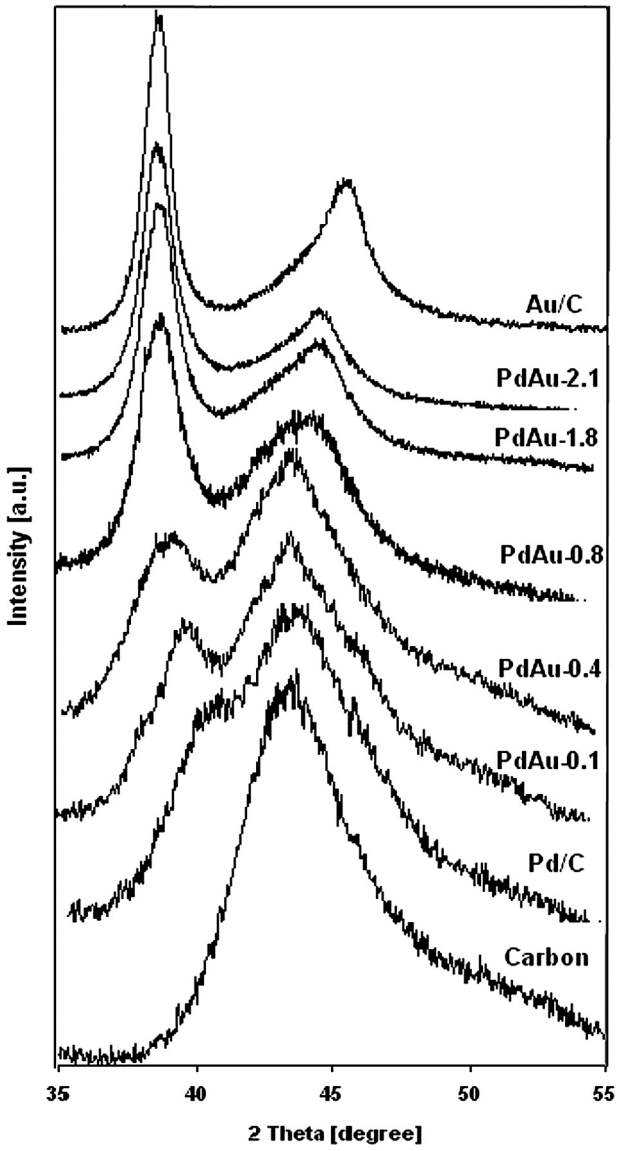

Fig. 1. XRD diffraction pattern of carbon support and carbon supported Pd/C, Au/C and PdAu/C catalysts.

The observed changes in textural properties (Table 1) suggest penetration of metal particles inside the carbon carrier. This could be related to the method of metal particles deposition. It was performed by contacting support with the microemulsion which predominantly consists of non-polar cyclohexane solvent. As described before, hydrophobic character of support favors chemical compatibility between the microemulsion and the support surface thus making more effective wetting of the support by the organic solvent and improves the distribution of the metal particles throughout the support grains.

The XRD diffraction patterns of studied catalysts are displayed in Fig. 1. In the diffraction pattern of 2%Au/C catalyst the intense diffractions at 2θ 38.16° and 44.3°, indexed to the (1 1 1) and (2 0 0) planes of face-centered cubic (fcc) crystalline Au, respectively appear. The latter diffraction (44.3°) is superimposed with that of carbon support. In the case of 2%Pd/C catalyst, the diffraction located at 2θ 40.16° indexed to (1 1 1) plane of face centered cubic (fcc) crystalline Pd can be seen. Although in both these catalysts metal loadings are the same, 2 wt%, the diffractions of gold are much more intense compared to that of palladium. This phenomenon is consistent with the results of Toshima et al. [4,5] who studied the monometallic Pd, Pt, Au and corresponding bimetallic Pd–Au, Pt–Au and Pd–Pt nanoparticles (all the particles of size in similar range). They were prepared by colloid-based method, namely ethanol reduction of metal ions in the presence of PVP. The obtained Pd particles gave the weakest XRD reflections whereas those of Pt were more intense and the Au particles gave the most distinct reflections. This effect has been also observed elsewhere and attributed to more amorphous structure of palladium particles.

In the diffraction patterns of PdAu/C catalysts, there are no diffractions arising from the crystalline Pd or Au components (Fig. 1). The diffraction peaks locate at 2θ intermediate between the Au (1 1 1) and the Pd (1 1 1), which is generally accepted to be an indication of PdAu alloy formation [5,8,39,50,51]. As the content of Au grows the observed diffraction is progressively shifted to lower angle relative to that of crystalline Pd. These XRD data indicate that the PdAu particles retained original (fcc) crystalline structure and gold is involved in alloying with palladium. A broad reflection at about 2θ = 43–44° associated with carbon can be seen in the patterns of all catalysts. However, as the content of Au increases the maximum of this broad diffraction is gradually shifted because of its superimposition with that arising from the (2 0 0) planes.

All diffraction peaks arising from metal particles are broad thus indicating the metal particles of size in nanoscale. The average particle size was calculated from the Pd (1 1 1) line broadening using the Scherrer equation. The obtained average metal particle sizes are given in Table 1.

The lattice parameter (a) is also calculated as described by other authors [51,52] (Supplementary Fig. S2). The addition of Au leads to an increase in the lattice parameter. Its growth is especially distinct at lower content of Au, up to Au/Pd = 0.8, after which relatively small change occurs. For PdAu-0.8 and PdAu-1.5, the lattice parameter increases only slightly from a = 4.02 Å to a = 4.06 Å although 2-fold growth in the Au content occurs. The latter value of a is only slightly lower than a = 4.086 Å, calculated for the monometallic Au/C catalyst.

The SEM images of monometallic and bimetallic catalysts together with corresponding particle size distributions diagrams are displayed in Figs. 2–4.

The Au/Pd atomic ratio was determined by the EDS analysis and the obtained data are collected in Table 1. They agree with the nominal data for studied PdAu/C catalysts, evidencing effective deposition of both metal components, Pd and Au, on the carbon support. It can be observed from the micrographs registered at low magnification (Fig. 2) that metal particles, even at high total metal loading as in the PdAu-1.8 catalyst (2 wt% Pd + 6.7 wt% Au) are well and almost uniformly distributed on the carbon support. In all catalysts the mono- as well as bimetallic particles all are spherically shaped, nearly monodispersed and the individual nanoparticles strongly predominate. However, some larger "white spots" of shapes suggesting aggregation of few individual spherical particles can be seen. This indicates that although aggregation of particles takes place during the deposition of metal particles onto carbon support, the contribution of this process is very low. The particle size distribution diagram was determined by measuring the size of over hundred particles from different areas in the SEM micrographs. The aggregated particles were omitted in the particle size analysis.

As shown in Fig. 3 Pd particles in the monometallic 2%Pd/C catalyst are nearly monodispersed with size in narrow range 4–9 nm giving the average Pd particles size d = 6.7 nm. The Au particles in the monometallic 2%Au/C catalyst are of larger size, d = 8.2 nm, and the size distribution is broader compared to Pd/C catalyst (Fig. 2). The results are consistent with previous data revealing that at the same parameter of "w" (at the same microemulsion composition) the size of particles varied being to some extent determined by the kind of metal Pd, Pt, Au [22]. The particle size distribution

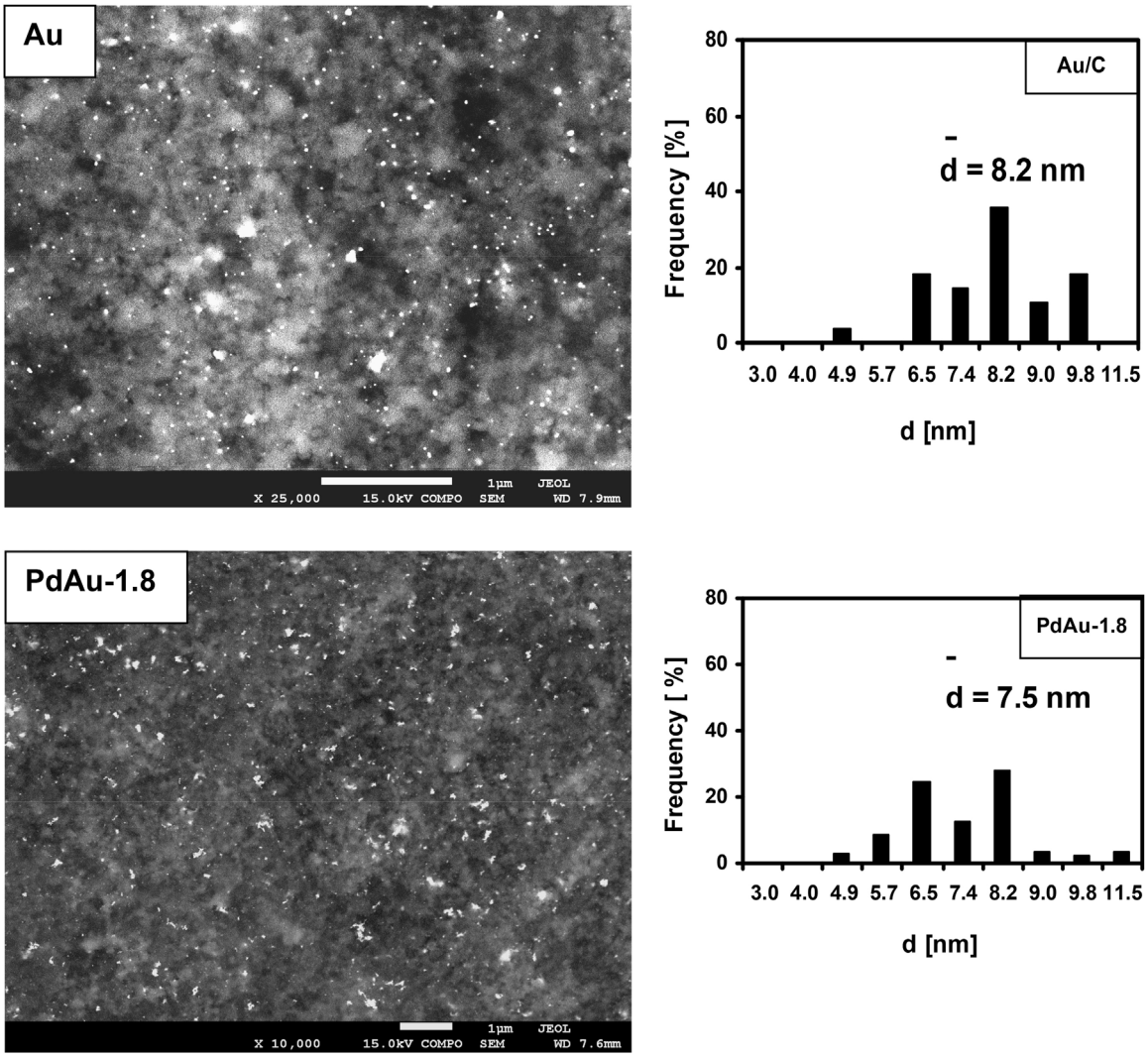

Fig. 2. SEM images and metal particles size distribution diagrams of 2%Au/C and PdAu-1.8 catalysts registered at magnification 25 000 and 10 000, respectively.

diagrams indicate that the size of metal particles is dependent on the Au/Pd ratio (Table 1). At low content of Au resulting in Au/Pd < 1, the particles have the average size smaller compared to that of monometallic Pd. When the Au/Pd molar ratio increases above Au/Pd = 0.8 and the content of Au is equal or higher than that of Pd, the size of particles gradually grows reaching 7.8 nm in the PdAu-2.1 catalysts vs 8.2 nm in the Au/C (Figs. 2 and 3). Moreover, at higher Au/Pd ratio, e.g. in Au-rich samples, the size distributions of particles are remarkably broader. The particles of size in the widest range and the largest average size (8.2 nm) can be seen in the monometallic 2%Au/C catalyst.

Thus, the average size of the bimetallic particles in the studied catalysts depends on the content of Au (Au/Pd ratio) and this relationship is displayed in Fig. 4. It should be pointed out that the size of metal particles calculated from the microscopic images agrees with those determined from the XRD diffractions. The relationship shown in Fig. 4 is consistent with previous results for the PdAu nanoparticles prepared by co-impregnation [39], adsorption–reduction [50] as well as colloid-based [4,5,21] methods. The colloidal bimetallic PdAu particles of Au/Pd molar ratio below 1 exhibited smaller size than the monometallic Pd or Au. However, at higher Au/Pd ratio (when the content of Au increased) the particles become larger reaching the size of monometallic Au [4]. Similar size-effect was observed for other bimetallic particles such as Pd–Pt, Pt–Au and it manifested especially distinctly for the latter Pt–Au nanoparticles [4,5]. This effect was discussed to arise from a specific role of individual metal components in the course of metal particles formation including nucleation and aggregation processes [50].

Selected PdAu/C catalysts are also subjected to the HRTEM studies to verify the alloy nature of the PdAu nanoparticles. Both the morphology and the composition of individual particles, chosen randomly, is also studied by the STEM attached to a high-resolution HRTEM. No particles composed of Pd or Au only were observed by the STEM in studied catalysts, with low as well as high Au/Pd ratios. The representative HRTEM images of catalysts with low Au content (PdAu-0.1, PdAu-0.4) are displayed in Fig. 5 and the micrographs of Au-rich (PdAu-1.8, PdAu-2.1) catalysts are shown in Supplementary Fig. S3. It is observed that the particles are single crystals with all the crystal lattices through the whole particle, indicating the alloy form of Pd and Au in the PdAu-2.1 catalyst.

The STEM analysis confirms the co-existence of both metals in the particles, with the average composition of individual particle which is roughly in agreement with the nominal contents of Pd and Au used in the synthesis. The obtained average data from the STEM analyses are collected in Table 1. However, the deviation of composition is observed among particles. It might result from very weak detection signal as well as from the detection errors because of very small size of the particles.

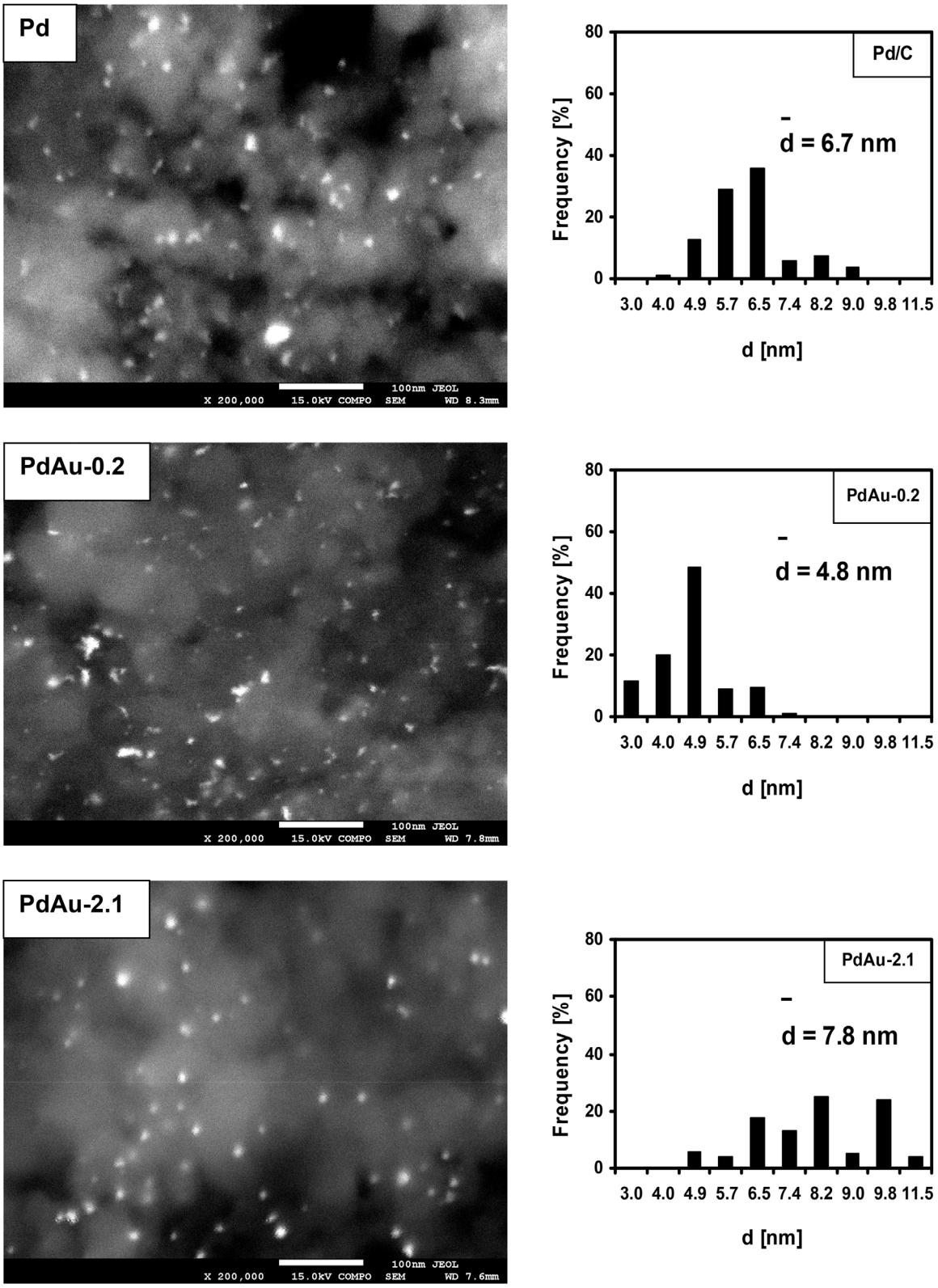

Fig. 3. SEM images and metal particles size distribution diagrams of 2%Pd/C and PdAu-0.2, PdAu-2.1 catalysts registered at magnification 200 000.

The catalysts were also subjected to the X-ray photoelectron spectroscopy (XPS) experiments. This technique showed the Pd, Au, C elements and traces of oxygen whereas no chloride was ascertained in outermost surface of studied catalysts. The obtained surface composition of Pd and Au (in at%) and the binding energies of palladium Pd $3d_{5/2}$ and Au $4f_{7/2}$ peaks are collected in Table 2. Here, the surface concentrations of palladium and gold estimated by XPS is taken into discussion, although it is well known that the depth of X-ray penetration might be up to 7–10 nm as it is to some extent influences by chemical composition (atomic number)

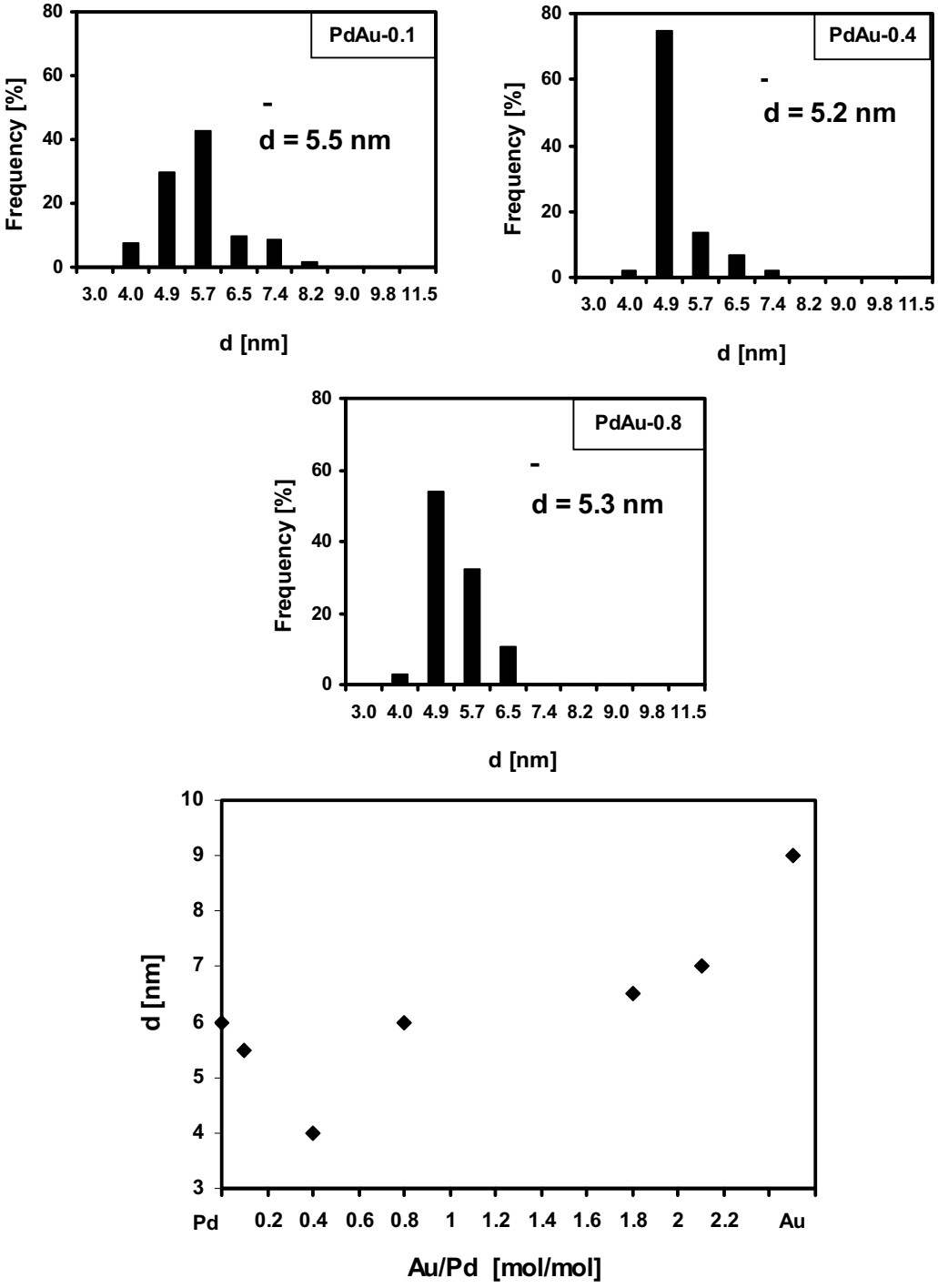

Fig. 4. Metal particles size distribution of PdAu-0.1, PdAu-0.4 and PdAu-0.8 catalysts and the relation between metal particle size and content of Au (Au/Pd ratio).

of analyzed surface components. Nevertheless, the data provided by this technique are widely considered to examine microstructure of bimetallic particles-containing supported catalysts.

The PdAu/C catalysts were prepared in such way, that the content of Pd was equal to 2 wt% whereas that of Au progressively grows from 0.4 wt% in PdAu-0.1 sample up to 7.8 wt% in the PdAu-2.1 catalyst. As shown in Table 2, the surface concentration of Au grows in line with increasing the Au/Pd ratio. The surface concentration of Pd is low and it is within similar range (0.05–0.07 at%) in the catalysts with lower Au/Pd ratio, up to PdAu-0.8. However, in both Au-rich catalysts, PdAu-1.8 and PdAu-2.1, the Pd surface concentration grows to 0.11–0.15 at% Pd, respectively. It should be pointed out that during deposition of pre-formed metallic nanoparticles on the carbon support the particles penetrated inside pore structure of carbon material. This penetration effect is reflected in the reduction of specific surface area accompanied by changes in the porous structure (Supplementary Fig. S1). On the other hand, the size of particles changed being determined by the Au/Pd ratio (Fig. 4). At Au content corresponding to Au/Pd > 0.8, the size of particles started to significantly grows. This could make their penetration more difficult thus giving higher surface concentration of Pd determined by XPS.

The XPS derived Au/Pd atomic ratio was calculated from the intensities of the Au and Pd peaks. However, at high Au-content

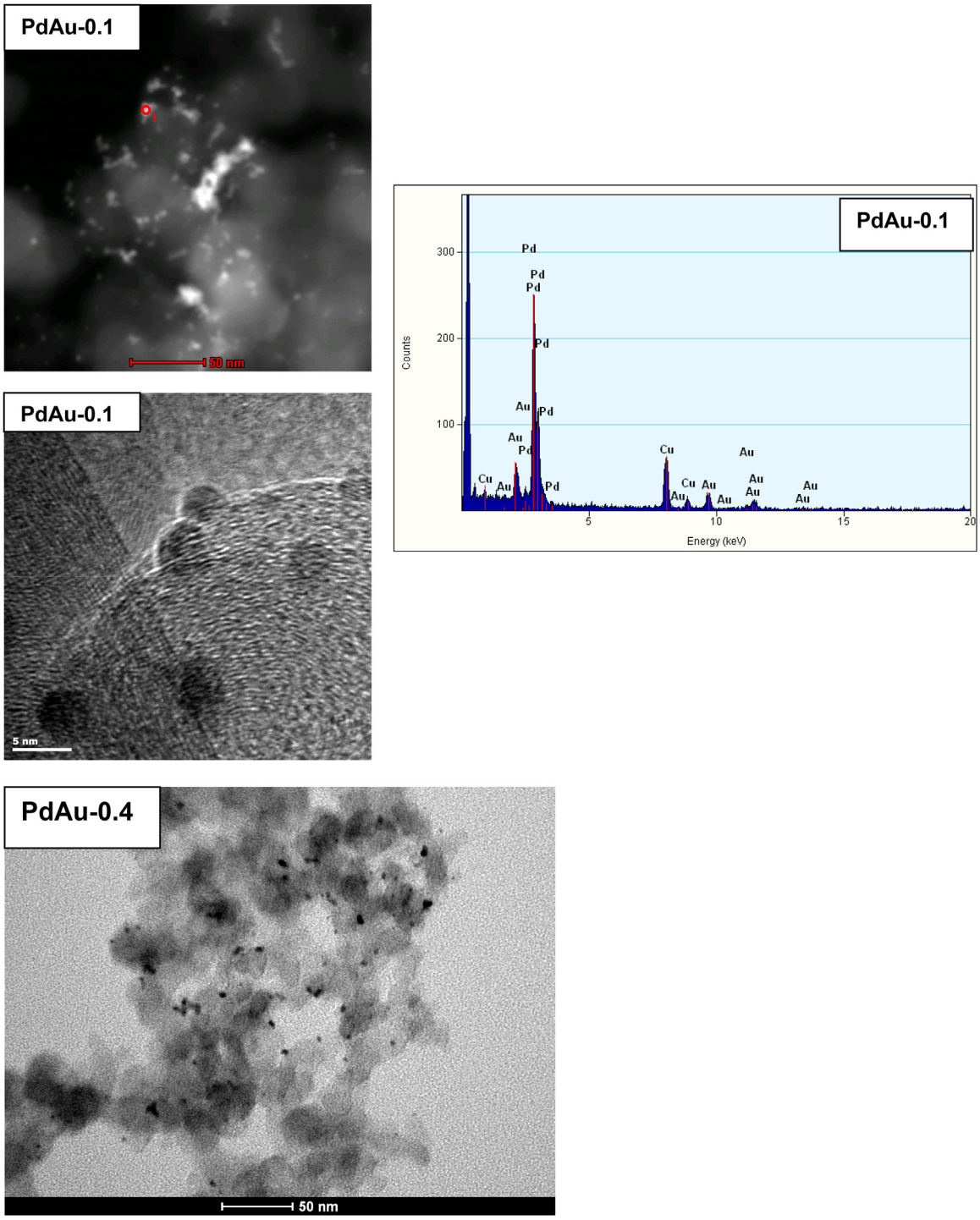

Fig. 5. Micrographs of catalysts with low Au content, PdAu-0.1 and PdAu-0.4 and electron diffraction spectrum for PdAu-0.1 catalyst.

this analysis was to some extent complicated because of some overlap between the Pd3d doublet and the Au $4d_{5/2}$ component. Therefore, the sensitivity factors were introduced and the calculated values are collected in Table 2. The Au/Pd atomic ratio determined by XPS in outermost surface is higher than the nominal value from the preparation. This shows the Pd-enrichment which is observed within the whole Au content. Even if the content of Au is higher than that of Pd as in the Pd–Au-1.8 and Pd–Au-2.1 catalysts the surface is enriched by Pd, what is evidenced by the Au/Pd molar ratio below 1. In the unsupported PdAu colloidal particles prepared by microemulsion method the surface of particles was also reported to be enriched by Pd [21].

The XPS data demonstrate the binding energy of Pd $3d_{5/2}$ within the range of 335–336 eV (Table 2). The peak component of binding energy at ca. 335 eV which is characteristic of metallic Pd [53] dominates in the spectra of all catalysts. In the spectrum of monometallic Pd/C catalyst the only Pd state of binding energy 335.3 eV corresponding to the Pd metal appears. In the spectra of all Au-containing catalysts the binding energy of Pd-metal peak component is slightly shifted (Supplementary Fig. S4). Moreover, the less intense peak component at slightly higher energy of ca. 336–337 eV appears.

Table 2
XPS data: surface concentration (at%), Pd $3d_{5/2}$ and Au $4f_{7/2}$ binding energies (eV), and the Au/Pd atomic ratio.

Catalyst	C	O	Pd	Au	Au/Pd atomic ratio	Au $4f_{7/2}$ [eV]	Pd $3d_{5/2}$ [eV]	
Pd/C			0.16				335.3	
Pd–Au-0.1	97.05	2.13	0.03	Trace		84.4	336.07 (0.51)*	337.1 (0.49)
Pd–Au-0.4	97.71	1.84	0.06	0.01	0.16	83.9	335.7 (0.53)	336.3 (0.47)
Pd–Au-0.8	95.51	3.99	0.05	0.02	0.40	84.6	335.7 (0.68)	337.5 (0.32)
Pd–Au-1.8	96.97	2.33	0.11	0.10	0.91	84.6	335.4 (0.59)	336.5 (0.41)
Pd–Au-2.1	97.07	2.35	0.15	0.13	0.87	84.5	335.5 (0.57)	336.9 (0.43)

* Contribution of energy state

The Pd binding energy values slightly above 336 eV are commonly ascribed to the partially oxidized Pd^{s+} species of lower electron density that Pd° or to the palladium in palladium oxide (336.5 eV) [54]. Thus, these spectral data could be an indication of Pd–Au electron interaction. The binding energies registered for gold are ca. 84.3 eV being typical of metallic Au [53].

The obtained Pd spectra are similar to those reported for supported PdAu catalysts prepared by other colloid-based methods, namely by simultaneous reduction of palladium and gold by ethanol in the presence of stabilizing polymer (PVP) [6,21].

3.2. Catalytic results

The catalytic hydrogenation of cinnamaldehyde (CAL) has been chosen to evaluate the catalytic properties of PdAu/C catalysts because this reaction is very sensitive to the surface properties of catalysts. In general, CAL has two functional groups, C=C and C=O, and their hydrogenation can lead to several products, namely hydrocinnamaldehyde (HCAL), cinnamyl alcohol (COL), 3-phenyl-1-propanol (HCOL) and the products of hydrogenolysis reaction, β-methyl, styrene and phenyl propane (PB) (Scheme 1). Palladium is known to exhibit especially high reactivity toward the unsaturated C=C bond hydrogenation yielding hydrocinnamaldehyde as the dominating product.

In the presence of all studied catalysts, the hydrocinnamaldehyde (HCAL) and saturated alcohol (HCOL) are formed from the very beginning of the reaction as the main products. Among hydrogenolysis products, phenyl propane (PB) is detected but its content is distinctly lower (2–8 mol%) compared to HCAL and HCOL. No cinnamyl alcohol (COL) is detected at the present hydrogenation conditions (toluene, 22 °C, atmospheric pressure of hydrogen) similarly to what was previously reported on Pd catalysts [55–58]. No other side products are detected.

Hammoudeh et al. [55] proved that in the hydrogenation of CAL on Pd/SiO_2 catalyst carried out at low temperature (25 °C) all saturated alcohol formed does entirely come through the consecutive hydrogenation of the cinnamyl alcohol. The experiments with COL as the substrate showed 30-times faster COL hydrogenation than the hydrogenation of CAL to cinnamyl alcohol [55,56]. A similar reactivity was also reported by Cairns et al. [57] for Pd/SiO_2 catalysts obtained by hydrogen reduction of $[Pd_2Br_4(PR3)_2]$. These catalysts were unable to reduce HCAL to saturated alcohol in decalin solvent at 135 °C whereas they readily converted cinnamyl alcohol to HCOL.

Based on these literature data, the control hydrogenation experiments are performed on 2%Pd/C and bimetallic PdAu-1.8 using HCAL as the substrate. On both catalysts, the hydrogenation of HCAL at 22 °C does not produce any detectable amount of saturated alcohol. The concentration of HCAL in the reaction mixture does not decrease and no consumption of hydrogen appears during catalytic tests lasting up to 4–6 h. Thus, in agreement with [55–57] at present mild reaction conditions (22 °C, atmospheric H_2 pressure) saturated alcohol HCOL is produced exclusively from the hydrogenation of COL as an initial step in the reaction.

The data in Table 1 show that the content of Au in the catalysts plays an important role in determining the course of CAL hydrogenation in terms of both, the rate and the selectivity control toward C=C/C=O hydrogenation. The selectivity data are discussed as the selectivity to either hydrocinnamaldehyde (HCAL) or fully saturated alcohol (HCOL). Although the content of PB was very low the selectivity to PB is also calculated.

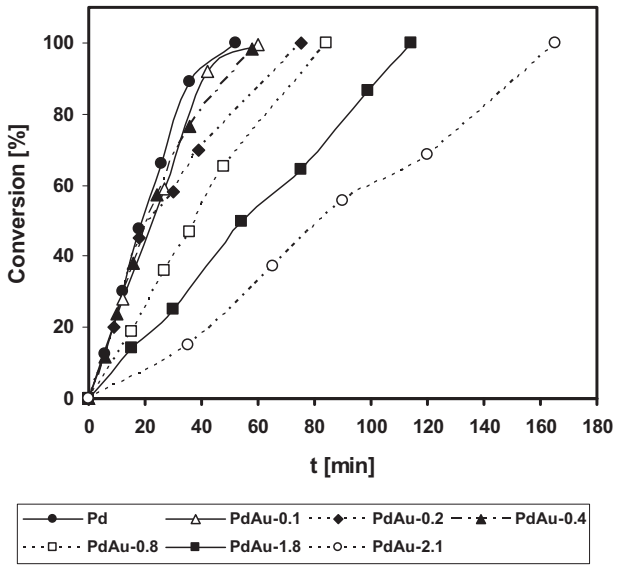

Fig. 6. Conversion of cinnamaldehyde against reaction time on monometallic Pd/C and bimetallic PdAu/C catalysts.

Among all studied catalysts, the monometallic 2%Pd/C exhibits the highest CAL conversion (Fig. 6) and the formation of HCAL exceeds that of fully saturated alcohol (HCOL) (Supplementary Fig. S5) giving the selectivity to HCAL as high as 65–70% (Fig. 7). This high selectivity to HCAL is almost preserved vs CAL conversion (Fig. 7). It is equal to ca. 70% in early stages of reaction and only slightly decreases as the CAL is reacted attaining ca. 65% at almost complete CAL conversion. For the 2%Au/C catalyst, the hydrogenation reaction did not proceed at present experimental conditions.

The activity of present 2%Pd/C catalyst could be compared with those of other Pd-catalysts in hydrogenation of CAL. Therefore the value of TOF (s^{-1}) expressed as the number of CAL moles converted per second and per surface Pd atom is calculated. From the size of Pd particles determined to be 6.7 nm (Table 1) the dispersion is calculated to be 16.7% which gives the TOF = 0.13 s^{-1}. This value could be compared with the literature data collected in Table 3. Apart from the TOF values also the conditions of CAL hydrogenation are reported (solvent, temperature H_2 pressure) because of their essential role in the activity. All the literature data concern reaction at temperature of 60 °C or higher and at H_2 pressure higher than 1 atm. On the other hand, temperature of 25 °C and H_2 pressure ca. 1 atm are the conditions in present catalytic tests. Nevertheless, it can be observed that TOF values are within wide range from 0.16 to 6.7 and they are determined not only by the metal particle size but also by the type of support. In the case of Pd/C catalysts the TOF values from 0.16 [59] up to 6.7 [60] can be observed. It should be

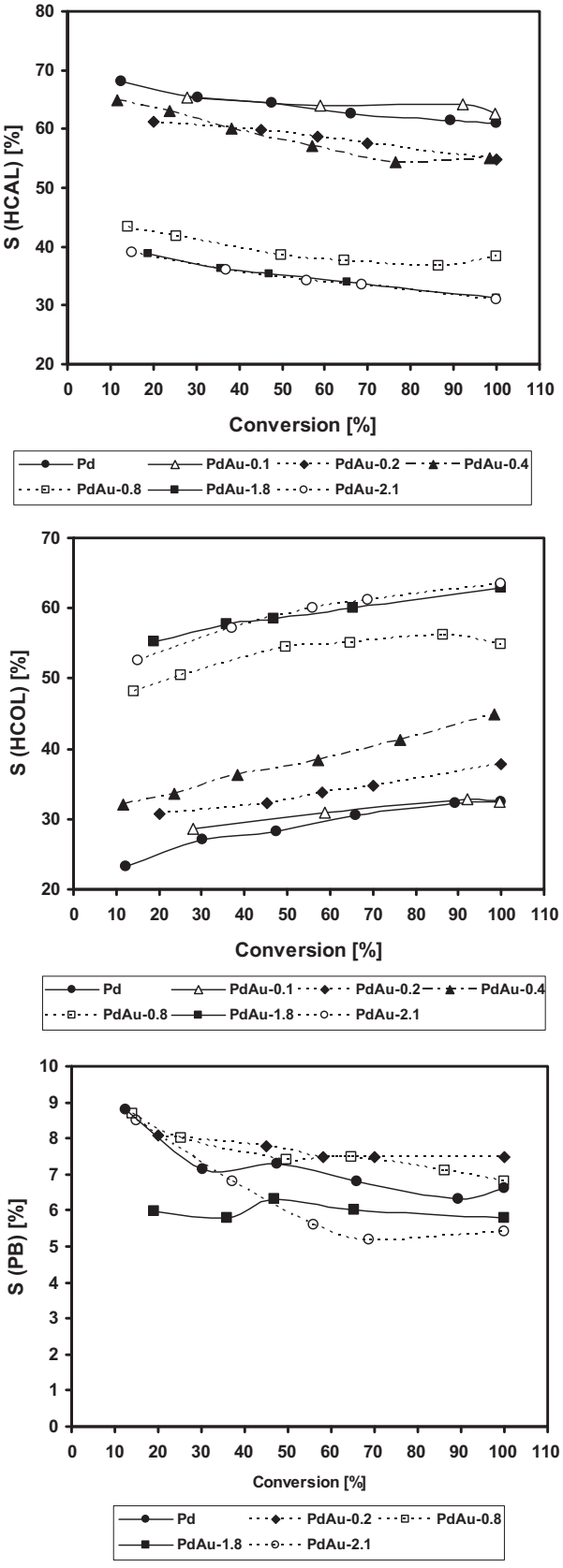

Fig. 7. Selectivity to saturated aldehyde (HCAL), saturated alcohol (HCOL) and propylobenzene (PB) vs conversion of cinnamaldehyde (CAL). Reaction carried out on Pd/C and PdAu/C catalysts. For reaction conditions, see Fig. 6.

stressed out that the selectivity control to C=C/C=O also remarkably varied. These carbon-induced effects have been discussed to be result of various influence of carbon material on the Pd (Pt) particles which is determined not only by textural and morphological features (micro, meso-porosity, nanofibers, nanotubes) but also by "carbon surface chemistry". The presence of oxygen-containing surface groups, their amount and the type (carboxyl, low or non-acidic such as hydroxyl) were observed to have a strong impact on the catalytic properties. According to Toebes et al. [64] the activity enhancement by a factor of 25 was reached at the expense of selectivity for the carbon nanofiber-supported Pt catalysts as a result of the thermal removal of oxygen groups. The reason is explained that the polarity changes of the catalyst surface due to removal of oxygen species influence the activity by modifying the preferential adsorption modes of CAL. Furthermore, the electronic effect induced by the carbon nanotubes due to differences in their curvatures was also found to have a strong impact on the catalyst performance [65]. The activity of present Vulcan XC72 supported catalyst (TOF = 0.13 s^{-1}) is lower compared to those of other catalysts given in Table 3, however, in contrast to the latter catalysts, this activity is determined at mild reaction conditions. Temperature increase from 20 to 60 °C results in ca. 3–4 fold increase in the activity. Nevertheless, the activity of present Pd/C catalyst is only slightly lower than that of Pd/CNT-TiO_2 catalyst (TOF = 0.16 s^{-1}) determined also in toluene solvent but at higher temperature (80 °C and H_2 pressure (2 MPa)) [59]. It can be assumed that the electroactive features of Vulcan XC72 carbon may play a role similarly to what was suggested by Sun et al. [41] from the comparison of catalytic performance of Au-based catalysts on various supports, among them Vulcan XC72 in CAL hydrogenation.

It is observed that as the Au content in the AuPd/C catalysts increases the hydrogenation activity is more or less reduced depending on the Au/Pd ratio. The relationships showing CAL conversion vs reaction time (Fig. 6) indicate that low Au content corresponding to Au/Pd < 0.8 does not significantly reduce activity of catalysts. All these catalysts exhibit high CAL conversions. However, at higher Au content a decrease in the rate of CAL conversion is distinct and the PdAu-2.1 catalyst with the highest Au/Pd ratio is about 5-times less active than monometallic Pd/C.

It must be noticed that all the catalysts studied contain a fixed percentage of 2 wt% Pd independently of the Au/Pd molar ratio. This results in an overall increase in the total metal concentration with growing Au content. In order to discuss a role of Au, initial activities are normalized per mole of metal (TOF_{IN}, min^{-1}) in the catalysts (Table 1) according to the procedure used in number of studies [1,2,9,43,44]. The obtained specific activities indicate that even the presence of a minor amount of Au (PdAu-0.1) reduces the activity of pure Pd and subsequent increase in the Au content leads to gradual decrease in the Pd activity. A role of the Au content in the reduction of Pd activity can be observed from the relationship between the decrease of initial hydrogenation activity (mol CAL min^{-1} g_{cal}^{-1}) referred to the number of Au moles vs the content of Au (mol%) in the catalysts (Supplementary Fig. S6). A very small amount of Au (9 mol%, PdAu-0.1) reduces Pd activity and as the Au content grows the reduction in Pd activity progressively grows up to the Au content ca. 40–45 mol%. At this composition corresponding to Au/Pd ~0.8–1 molar ratio the decrease in Pd activity is the highest. Larger amount of Au corresponding to Au/Pd > ~1 also reduces activity of Pd but to lesser extent. It may be speculated from this tendency that further growing of Au content at a fixed Pd loading leading to Au/Pd ≫ 1 may result in the PdAu particles of activity comparable or even higher than that of Pd. This may suggest a system consisting of Au in excess relative to that of Pd. In fact, the nanostructured PtAu/SiO_2 catalysts composed of fully dispersed Pt-entities onto the surface of Au nanoparticles were observed to

Table 3
The comparison of TOF data reported in the literature.

Conditions of CAL hydrogenation experiment	Catalyst	Pd [nm]	TOF [s^{-1}][a]	Ref.
2-Propanol/water; 60 °C; 4 MPa H_2 pressure	Pd/graphite[A]		6.7	[60]
Cyclohexane; 60 °C; 1 MPa H_2 pressure	Pd/C activated carbon	2.8–8.5	2.8–3.3 90% HCAL; irrespective of Pd-particle size	[61]
Ethanol; 60 °C; 0.2 MPa H_2 pressure	Pd/C, commercial	3.3	1.4 70% HCAL; 30%HCOL	[62]
Toluene, 80 °C; 2 MPa H_2 pressure	0.5%Pd/FAC activated carbon	2.8	0.25	
	Pd/MC mesoporous carbon	3.5	0.23	
	Pd/CNF carbon nanofiber, powdered	5.6	0.20	[59]
	Pd/CNF/TiO_2 carbon nanofiber-wash coated TiO_2-monolith-	7.8	0.16	
	Pd/CNF/TiO_2 carbon nanofiber-washcoated TiO_2 monolith	8.2	0.21	
2-Propanol, 60 °C; 1 MPa H_2 pressure	Pd/Al_2O_3	3	0.3–0.5	
		7	0.3	
		28	1.9	[63]
	Pd/SiO_2	4	0.3	
		54	3.4	

[a] The turnover frequency (TOF), number of CAL molecules converted per second and per surface Pd atom.

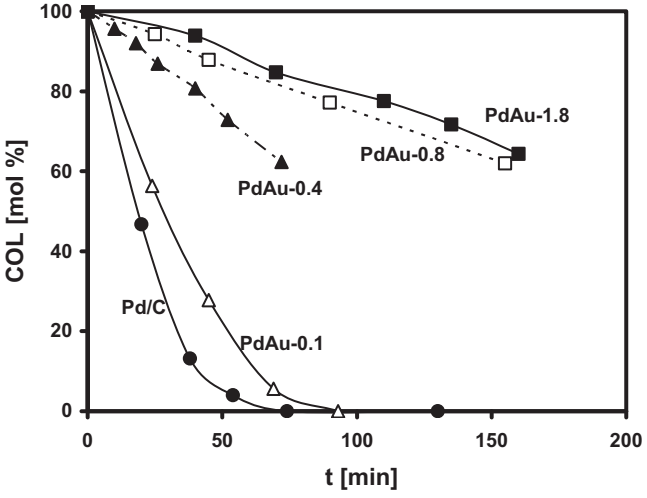

Fig. 8. The influence of Au content in the PdAu/C catalysts on cinnamalcohol (COL) hydrogenation. Reaction conditions: toluene, temperature 22 °C, catalyst concentration 0.25 g/dm^3, substrate COL concentration c^0 = 0.05 mol/dm^3.

be very active for the hydrogenation of α,β-unsaturated carbonyl compounds (CAL, furfural) [41,66].

An addition of Au has also an impact on the way CAL is reacted (Fig. 7). In comparison with Pd/C, the changes in selectivity are not so much strong on catalysts with low Au content, when Au/Pd is below 0.8, and the hydrogenation of C=C predominates over the carbonyl group hydrogenation. However, with increasing Au/Pd ratio from 0.1 to 0.4 a clear tendency reflecting in progressively growing selectivity to saturated alcohol is observed. The selectivity to saturated alcohol increases dramatically at the expense of that to saturated aldehyde on Au-rich catalysts, when Au/Pd > 0.8. On both Au-rich catalysts the selectivity to saturated alcohol (HCOL) attains ca. 60% (vs 30% on Pd/C catalyst) whereas that to saturated aldehyde HCAL is only 40% (compared to 65% on Pd/C). In their presence the content of saturated alcohol (HCOL) exceeds that of saturated aldehyde (HCAL) during the whole CAL conversion (Supplementary Fig. S5). The Au-content has also slight impact on the hydrogenolysis reaction yielding propyl benzene (PB) (Fig. 7). On Au-rich catalysts the ability to PB formation is somewhat smaller when compared with small Au content – containing catalysts.

Next series of hydrogenation tests are performed using COL as the substrate. They allow to compare reactivity of active sites in monometallic Pd/C and PdAu/C catalysts for the hydrogenation of isolated C=C bond of COL reactant (Fig. 8). On all Pd/C and PdAu/C catalysts, the saturated alcohol (HCOL) was formed with selectivity higher than 98%. No isomerization to HCAL was noted, and the formation of hydrogenolysis product, PB was also very low. The monometallic 2%Pd/C catalyst has the highest activity while all Au-containing catalysts are less active and at Au/Pd > 0.8 activity drops drastically. Thus, the adsorption of isolated C=C bonds of COL reactant occurs on Pd as well as PdAu catalysts, but the presence of Au strongly reduces reactivity to isolated C=C bond hydrogenation, especially in the case of Au-rich catalysts.

In next series of experiments, the hydrogenation was studied using a mixture of CAL and unsaturated alcohol, COL (10 mol% COL relative to CAL) on monometallic 2%Pd/C and Au-rich PdAu-1.8 catalyst. An affect of added COL on their reactivity can be compared from graphs in Fig. 9. The hydrogen consumption curves and the reactants distribution profiles show that on both studied catalysts COL is preferentially reduced from the very beginning of the experiment. This is evidenced by almost complete decrease of COL content in the early stage of both reactions. It is also reflected by a distinct break (indicated by the arrows in Fig. 9) on the hydrogen consumption curves at the reaction time corresponding to the complete conversion of COL. It is also observed that added COL reduces the rate of CAL conversion on both Pd/C and PdAu-1.8 catalysts. In the presence of added COL the selectivity to HCAL is greatly diminished on Pd/C catalyst while it does not essentially change on Au-rich PdAu-1.8 catalyst. Similar activity/selectivity effect due to added COL observed on Ir/C catalyst was explained by a competitive adsorption of COL with starting aldehyde (CAL) [67]. This competitively adsorbed COL created a steric effect that inhibited the planar adsorption of CAL (involving both C=C and C=O bonds) and limited the formation of HCAL. A competitive adsorption of unsaturated alcohol with the unsaturated aldehyde on Pt, Pd catalysts was proved by the theoretical DFT calculation [68,69]. They showed preferential adsorption of unsaturated alcohol through a vertical atop geometry. On the other hand, saturated aldehyde can not compete with the starting unsaturated aldehyde. Thus, COL can alter the way in which the reactant (CAL) binds to the catalyst surface. With increasing surface coverage of the COL (added or formed during the reaction) the CAL becomes more hindered to flat adsorption thus preventing the hydrogenation of C=C bond yielding saturated aldehyde. This effect can be clearly seen on Pd/C catalyst (Fig. 9). However, there is no essential change in the selectivity to HCAL on the PdAu-1.8 catalyst which itself offers distinctly lower ability to HCAL formation because of less favorable planar mode of CAL adsorption.

Here, the stability of PdAu/C catalysts under CAL hydrogenation reaction is also examined. In order to assess the stability of catalysts, recycle tests were conducted using PdAu-0.1 and

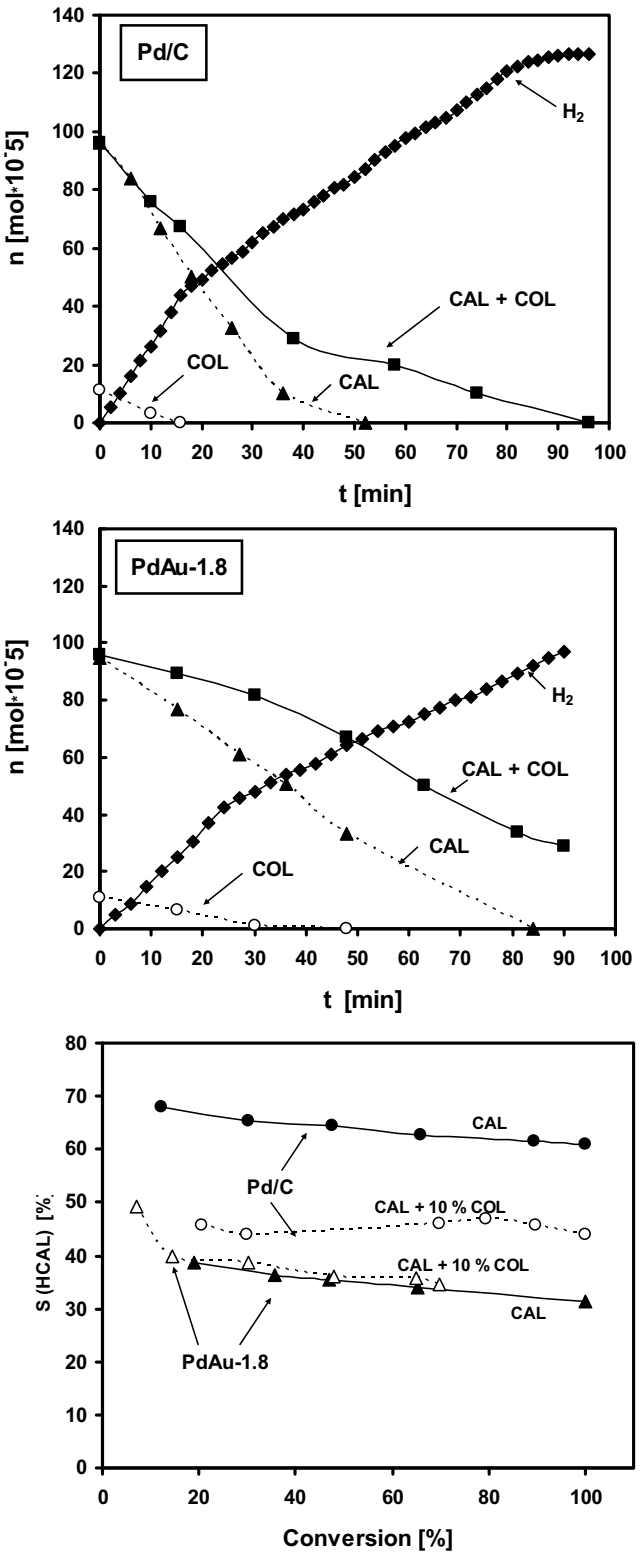

Fig. 9. The effect of added COL on the CAL hydrogenation in the presence of Pd/C and PdAu-1.8 catalysts. Products distributions profiles and selectivity to saturated aldehyde (HCAL). Reaction carried out on monometallic Pd/C and Au-rich PdAu-1.8 catalysts. Reaction conditions: toluene, temperature 22 °C, catalyst concentration 5 g/dm^3, CAL concentration c^0 = 0.05 mol/dm^3, initial COL concentration c^0 = 0.005 mol/dm^3.

PdAu-2.1 catalysts as follows: at the end of the first hydrogenation run the catalyst was filtered off, washed with acetone-THF (1:1) mixture and after drying in air was reused for the next reaction under the same conditions. The reuse of both PdAu/C catalysts recovered from the reaction mixture leads to almost reproducible results in terms of both activity and selectivity (Supplementary Fig. S7). The conversion remained stable during second cycle, and the selectivity did not change essentially. Thus it is rational to conclude about promising stability of studied PdAu/C catalysts under used reaction conditions.

Thus, the surface composition exhibits significant role in catalytic behavior of PdAu/C catalysts not only in activity but also in the C=C/C=O selectivity control in hydrogenation of CAL especially in the case of Au-rich catalysts when the surface concentration of Au is equal or even exceeds that of Pd (Table 2). 2%Au/C catalyst does not exhibit activity at the present reaction conditions. The reason could be the low capacity of gold to dissociate H_2 which only occur on gold surface defects (corners, kinks, etc.) [70]. Therefore, palladium could be considered to be essential in the hydrogenation of CAL while the presence of gold assists the catalytic function of palladium.

Similar effect, gradual decrease in the rate of C=C hydrogenation in 1,3-cyclooctadiene with growing Au content observed on colloidal PdAu nanoparticles prepared by co-reduction (ethanol) in the presence of PVP has been related to the presence of Au on the surface since the activity in the C=C hydrogenation could be expected to be proportional to the number of surface Pd atoms [3–5]. The surface composition of Au and Pd is according to the authors determined by the nominal Au/Pd ratio with is decisive for the type of microstructure existing in the PdAu particles. Simultaneous reduction (alcohol) at low temperature could produce so-called core–shell structure resulting due to difference in the reduction ability of Pd and Au. Since the reduction potential of Au ions is more positive (E° (Au^{3+}/Au) = + 1.0 V vs NHE) than that of Pd ions (E° (Pd^{2+}/Pd) = + 0.63 V vs NHE) the reduction of the Au ions proceeds more easily than that of the Pd ions and the core is Au-rich while surface shell is enriched by Pd. However, various microstructures such as Au-core/Pd-shell, cluster-in-cluster or random model could be formed as they are determined by the Au/Pd ratio [5]. The most active catalyst was identified to be Au/Pd = 1:4 (PdAu-0.25 in the present notation) with the surface shell entirely composed of Pd atoms and a core composed of Au. It exhibited enhanced activity due to electron interaction between the Au-core and the surface shell Pd atoms. At higher Au content the cluster-in-cluster or random models could be formed in which both, Pd and Au atoms but in different relations could appear in the surface shell. This implied that the presence of Au atoms on the surface of colloidal AuPd particles resulted in lower activity for C=C hydrogenation in 1,3-cyclooctadiene [4,5]. The same model has been adopted to explain the mechanism of PdAu, PdPt and PtAu nanoparticles formation by reverse "water-in-oil" microemulsion method [20–22]. Number of techniques demonstrated no-complete "core–shell" structure of colloidal PdAu, PdPt, PtAu particles formed at these conditions. In the case of PdAu particles, both Pd and Au were detected in outer surface of colloidal particles within wide range of composition. Hence, in view of such literature, a microstructure of metal particles in the present PdAu/C catalysts may be considered to be no-complete "core–shell" structure with both Au and Pd in their outer surface. Consequently, as the surface content of Au grows the hydrogenation activity of PdAu/C catalysts gradually decreases. However, this growing surface content of Au has an essential impact on the selectivity of CAL hydrogenation. The selectivity to C=O is remarkably promoted especially when the Au content is comparable or higher than that of Pd. At Au/Pd > 1 the HCAL formation is so strongly inhibited that the formation of saturated alcohol is a dominating reaction. This may suggest a role of Au

in the surface Au-rich catalysts in the geometry of CAL adsorption, the phenomenon which is commonly taken into account to discuss the selectivity effects theoretically studied by Delbecq et al. [68,69]. The aldehyde reactant can be adsorbed on a metal surface in a flat, planar adsorption mode, parallel to the surface with both C=C and C=O bonds involved in adsorption and in a vertical (atop) geometry via interaction with the surface by the oxygen atom (C=O). The first adsorption mode favors the hydrogenation of C=C yielding HCAL, while atop geometry promotes the formation of unsaturated alcohol. Moreover, the CAL molecule contains a large phenyl group, which can have a considerable steric effect. Because of repulsion between metal and aromatic ring the parallel adsorption of CAL molecule on metal surface could be to high extent hindered.

It is well known that the addition of second metal acting as a modifier can result in an increasing as well as a decreasing activity. The presence of ionic promoters directing the C=O bond toward the active sites, enhanced not only selectivity to unsaturated alcohol but also the activity. Decreased activities have been ascribed to the presence of high promoter concentrations resulting in a dramatically decreasing hydrogenation capacity. For instance addition of Ga, Sn and Ge improves selectivity whereas the activity decreased [37]. The latter was also the case in the hydrogenation of CAL in the presence of Sn-modified Pd/SiO_2 [55] and Pd/C catalysts [71]. The decreased activity was related to lower number of active sites because of Sn addition. Furthermore, as the content of Sn in the $Pd\text{-}Sn/SiO_2$ catalysts increased, their activity decreased accompanied by a promotion of selectivity toward COL. From these results the authors concluded about the changes in adsorption mode of CAL due to electronic and geometric effects induced by the Sn. The promotion of C=O selectivity on present PdAu/C catalysts is also accompanied by the reduced activity especially on the Au-rich catalysts. At Au/Pd > 1 the HCAL formation is so strongly inhibited that the formation of saturated alcohol is a dominating reaction (Supplementary Fig. S5).

Therefore, the change of adsorption mode of CAL on Pd surface induced by Au could be considered to be a main reason for the enhanced selectivity toward COL. It can be supposed that when the Au/Pd ratio grows, e.g. on the Au-rich surface the possibility of flat-lying CAL adsorption mode becomes more and more inhibited. Core-level XPS spectra indicate an electronic perturbation of palladium by gold (Supplementary Fig. S4) which may modify the Pd sites both geometrically and electronically. However, these interaction may also provide new active sites which are able to active the C=O bond of CAL. The role of geometric dilution effect of Pd atoms by alloyed Au could also be taken into consideration. Dividing the Pd ensembles by Au into ensembles of smaller sizes would prevent the CAL adsorption in the "parallel" mode that requires multi-adsorption sites with consequent improving the selectivity toward C=O hydrogenation [55].

The metal particle size is another feature which could enhance the selectivity toward unsaturated alcohol and larger particles of Pt, Pd, Ru, Co, resulted in higher selectivity to C=O hydrogenation [37]. The effect of metal particle size was related to the phenyl group, sterically hindering the approach of the C=C moiety to the surface of large particle leading to the preferential adsorption of C=O. This selectivity improvement is due to the lower probability of the C=C bond activation rather than to an increased activation of the C=O bond. The size of metal particle increases in the PdAu/C catalysts in particular for Au-rich catalysts, e.g. when the Au/Pd > 0.8. Thus, it cannot be excluded that such metal particle size effect could also contribute to the catalytic performance of studied PdAu/C catalysts.

The benefit brought by alloying Pd–Au in the PdAu/silica catalysts with low Au content (Au/Pd molar ratio of 0.2:1) was recognized to be enhanced activity as compared with Pd-catalyst whereas it did not essentially change the selectivity of CAL hydrogenation [39]. Hydrogen spillover effect acting on nanostructured Pt-on-Au catalysts [40,41] and on a physical mixture of TiO_2 supported Au and Pd catalysts [43] improved also strongly the activity, but it exhibited tendency to facilitate the C=C hydrogenation yielding higher selectivity to saturated aldehyde (HCAL) [44].

In summary, the reverse "water-in-oil" microemulsion method proves to be successful in the preparation of carbon supported catalysts with dispersed and almost homogeneously distributed PdAu nanoparticles with narrow size distributions. The PdAu particles in studied catalysts exhibited alloy structure and within the whole Au/Pd ratios both components Pd and Au are detected in their outer surface. The surface composition of these particles particularly in Au-rich catalysts played a role in the CAL molecule adsorption resulting in enhanced selectivity to carbonyl group hydrogenation.

On the other hand, it is well known that Pd–Au synergistic effect observed by Yang et al. [39] is strongly dependent on the nanostructure of bimetallic AuPd particles which may vary depending on the method of preparation [72]. In particular thermal treatment could play an important role as it facilitates an intermixing process of Pd and Au components which may lead to restructuring of surface composition of metal particles. It could also have a clear impact on the chemical state and mutual interaction between the components, e.g. Pd and Au [73].

In the present work the PdAu/C catalysts were neither calcined nor hydrogen treated at high temperature after deposition of pre-formed PdAu colloidal particles on the carbon support. The preparation protocol described by Wu et al. [21] was preserved and the PdAu/C catalysts were dried at temperature of 120 °C only. It could be not excluded that thermal treatment would modify microstructure of these PdAu/C catalysts because of an expected thermally induced Pd–Au intermixing effect, similarly to what was observed by Sarkany et al. [74] for colloidal PdAu nanoparticles deposited on SiO_2 and studied in the hydrogenation of acetylene. The intermixing of Au and Pd upon thermal treatment significantly enhanced the hydrogenation activity explained by thermally facilitated generation of gold diluted Pd–Au ensembles.

4. Conclusions

The liquid phase hydrogenation of cinnamaldehyde was studied on carbon (Vulcan XC72) supported PdAu catalysts with Au/Pd atomic ratio from 0.1 up to 2.1 prepared by colloid-based reverse "water-in-oil" microemulsion method. Accordingly, pre-formed metal nanoparticles of controlled size with a narrow size distribution were deposited on the carbon support. In all catalysts the metal particles are spherically shaped, nearly monodispersed and well distributed throughout the carbon support. The size of metal particles was dependent on the Au-content expressed by the Au/Pd ratio. The particles of low Au-content (Au/Pd < 0.8) are of smaller size than Pd (6.7 nm), but the particle size increases and at Au/Pd = 2.1 it is only slightly lower than that of Au (8.2 nm).

The content of Au (Au/Pd ratio) has impact on activity and selectivity for the cinnamaldehyde hydrogenation. The C=C group of cinnamaldehyde was preferentially hydrogenated compared to the carbonyl (C=O) group in the presence of Pd/C catalyst. At low Au content (Au/Pd < 0.8) the effect of Au was relatively weak observed as a small decrease in activity with only small increase in selectivity to C=O hydrogenation. The effect of Au manifested strongly on Au-rich catalysts (Au/Pd > 1) giving distinctly reduced reactivity to unsaturated double C=C bond hydrogenation and selectivity preference to the carbonyl group reduction C=O. The change of adsorption mode of CAL on the surface could be the main reason of significantly limited C=C adsorption on Au-rich catalysts. These activity/selectivity effects induced by the presence of Au are discussed to arise from microstructure of PdAu alloy particles which

manifests distinctly in various surface concentrations of Au relative to that of Pd. It can be supposed that when the Au/Pd ratio is high, e.g. on the Au-rich surface the possibility of cinnamaldehyde molecule adsorption in a "flat-lying CAL" geometry becomes more and more inhibited. Core-level XPS spectra indicate electronic perturbation of palladium by gold. It might be thought that the Pd–Au interactions modify the Pd sites both geometrically and electronically and it resulted in significantly limited C=C bond adsorption. However, these interaction may also provide new active sites which are able to active the C=O bond of CAL.

Acknowledgements

This work was partially supported by the National Centre for Research and Development, Poland, Grant no. SP/J/7/170071/12. We are grateful to Dr Elżbieta Bielańska for taking SEM images and Prof. Lidia Lityńska-Dobrzyńska for registering HRTEM images.

Appendix A. Supplementary data

Supplementary data associated with this article can be found, in the online version, at http://dx.doi.org/10.1016/j.apcata.2014.08.036.

References

[1] J.A. Lopez-Sanchez, N. Dimitratos, N. Glanville, L. Kesavan, C. Hammond, J.K. Edwards, A.F. Carley, Ch.J. Kiely, G.J. Hutchings, Appl. Catal. A 291 (2011) 400–406.
[2] N.E. Kolli, L. Delannoy, C. Louis, J. Catal. 297 (2013) 79–92.
[3] N. Toshima, M. Harada, Y. Yamazaki, K. Asakura, J. Phys. Chem. 96 (1992) 9927–9933.
[4] T. Yonezawa, N. Toshima, J. Chem. Soc. Faraday Trans. 91 (1995) 4111–4120.
[5] N. Toshima, T. Yonezawa, N. J. Chem. (1998) 1179–1201.
[6] A.M. Venezia, V. La Oarola, D. Deganello, B. Pawelec, J.L.G. Fierro, J. Catal. 215 (2003) 317–325.
[7] A.M. Venezia, L.F. Liotta, G. Pantaleo, V. La Parola, G. Deganello, A. Beck, Z. Koppany, K. Frey, D. Horvath, L. Guczi, Appl. Catal. A 251 (2003) 359–368.
[8] B. Pawelec, A.M. Venezia, V. La Parola, E. Cano-Serrano, J.M. Campos-Martin, J.L.G. Fierro, Appl. Surf. Sci. 242 (2005) 380–391.
[9] J. Pritchard, L. Kesavan, M. Piccinini, Q. He, R. Tiruvalam, N. Dimitratos, J.A. Lopez-Sanchez, A.F. Carley, J.K. Edwards, Ch.J. Kiely, G.J. Hutchibs, Langmuir 26 (2010) 16568–16577.
[10] S. Marx, F. Krumeich, A. Baiker, J. Phys. Chem. C 115 (2011) 8195–8205.
[11] M. Boutonnet, S. Logdberg, E.E. Svensson, Curr. Opin. Colloid Interface Sci. 13 (2008) 270–286.
[12] M.J. Schuger, K. Stickdorn, Chem. Rev. 95 (1995) 849–864.
[13] S. Erikson, U. Nylen, S. Rojas, M. Boutonnet, Appl. Catal. A: Gen. 265 (2004) 207–219.
[14] H.H. Ingelsten, J.-C. Beziat, K. Bergvist, A. Palmqvist, M. Skoglundh, H. Quiuhong, L.K.L. Falk, K. Holmerg, Lamgmuir 18 (2002) 1811–1818.
[15] J. Rymes, G. Ehret, L. Hilaire, M. Boutonnet, K. Jiratova, Catal. Today 75 (2002) 297–303.
[16] A. Martinez, G. Prieto, Catal. Commun. 8 (2007) 1479–1486.
[17] A. Martinez, G. Prieto, J. Catal. 245 (2007) 470–476.
[18] R. Kosydar, M. Góral, J. Gurgul, A. Drelinkiewicz, Catal. Commun. 22 (2012) 58–67.
[19] M. Góral-Kurbiel, A. Drelinkiewicz, R. Kosydar, B. Debinska, P.J. Kulesza, J. Gurgul, Electrocatalysis 5 (2014) 23–40.
[20] M.-L. Wu, D.-H. Chen, T.-C. Huang, Chem. Mater. 13 (2001) 599–606.
[21] M.-L. Wu, D.-H. Chen, T.-C. Huang, Langmuir 17 (2001) 3877–3883.
[22] M.-L. Wu, D.-H. Chen, T.-C. Huang, J. Colloid Interface Sci. 243 (2001) 102–108.
[23] Z. Liu, J.Y. Lee, M. Han, W. Chen, L.M. Gan, J. Mater. Chem. 12 (2002) 2453–2458.
[24] L. Xiong, A. Manthiram, Electrochim. Acta 50 (2005) 2323–2329.
[25] S. Devarajan, P. Bera, S. Sampath, J. Colloid Interface Sci. 290 (2005) 117–129.
[26] U. Nylen, J.F. Delgado, S. Jaras, M. Boutonnet, Appl. Catal. A 262 (2004) 189–200.
[27] R. Touroude, P. Girard, G. Maire, J. Kizling, M. Boutonnet-Kizling, P. Stenius, Colloid Surf. 67 (1992) 9–12.
[28] S.J. Chiang, B.J. Liaw, Y.Z. Chen, Appl. Catal. A 319 (2007) 144–152.
[29] B.A. Cheney, J.A. Lauterbach, J.G. Chen, Appl. Catal. A 394 (2011) 41–47.
[30] A. Di Wang, F. Villa, L. Porta, D.S. Prati, J. Phys. Chem. C 112 (2008) 8617–8622.
[31] D.I. Enache, J.K. Edwards, P. Landon, B. Solsona-Espira, A.F. Carley, A.A. Herzing, M. Watanabe, C.J. Kiely, D.W. Knight, G.J. Hutchings, Science 311 (2006) 362–365.
[32] M. Bonarowska, J. Pielaszek, V.A. Semikolevov, Z. Karpiński, J. Catal. 209 (2002) 528–538.
[33] A. Sarkany, A. Horvath, A. Beck, Appl. Catal. A 229 (2002) 117–125.
[34] A. Sarkany, O. Geszti, G. Safran, Appl. Catal. A 350 (2008) 157–163.
[35] A.C. Krauth, G.H. Bernstein, E.E. Wolf, Catal. Lett. 45 (1997) 177–186.
[36] G. Schmid, A. Lehnert, J.O. Halm, J.O. Bovin, Angew. Chem. Int. Ed. Engl. 30 (1991) 873–874.
[37] P. Gallezot, D. Richard, Catal. Rev. Sci. Eng. 40 (1998) 81–126.
[38] P. Maki-Arvela, J. Hajek, T. Salmi, D.Y. Murzin, Appl. Catal. A 292 (2005) 1–49.
[39] X. Yang, D. Chen, S. Liao, H. Song, Y. Li, Z. Fu, Y. Su, J. Catal. 291 (2012) 36–43.
[40] Y.C. Hong, K.Q. Sun, G.R. Zhang, R.Y. Zhong, B.Q. Xu, Chem. Commun. 47 (2011) 1300–1302.
[41] K.Q. Sun, Y.C. Hong, G.R. Zhang, B.Q. Xu, ACS Catal. 1 (2011) 1336–1346.
[42] H. Shi, N. Xu, D. Zhao, B.Q. Xu, Catal. Commun. 9 (2008) 1949–1954.
[43] R. Liu, Y. Yu, K. Yoshida, G. Li, H. Jiang, M. Zhang, F. Zhao, S. Fujita, M. Arai, J. Catal. 269 (2010) 191–200.
[44] H. Gu, X. Xu, A. Chen, P. Ao, X. Yan, Catal. Commun. 41 (2013) 65–69.
[45] E. Antolini, E.R. Gonzales, Appl. Catal. A 365 (2009) 1–19.
[46] A. Drelinkiewicz, A. Waksmundzka, W. Makowski, J.W. Sobczak, A. Król, A. Zieba, Catal. Lett. 94 (2004) 143–156.
[47] A. Drelinkiewicz, M. Hasik, J. Mol. Catal. A 177 (2001) 149–164.
[48] S. An, J.-H. Park, C.-H. Shin, J. Joo, E. Ramsaamy, J. Hwang, J. Lee, Carbon 49 (2011) 1108–1117.
[49] R. Sellin, J.-M. Clacens, C. Coutanceau, Carbon 48 (2010) 2244–2254.
[50] X. Wei, X.F. Yang, A.Q. Wang, L. Li., X.Y. Liu, T. Zhang, C.Y. Mou, J. Li, J. Phys. Chem. C 116 (2012) 6222–6233.
[51] G. Zhang, Y. Wang, X. Wang, Y. Chen, Y. Zhou, Y. Tang, L. Lu, J. Bao, T. Lu, Appl. Catal. B 102 (2011) 614–619.
[52] A.F. Lee, C.J. Baddeley, C. Hardacre, R.M. Ormerod, R.M. Lambert, J. Phys. Chem. 99 (1995) 6096–6102.
[53] NIST Standard Reference Database 20, Version 3.2 (Web Version), National Institute of Standards and Technology, Gaithersburg, 2001.
[54] T. Kobayashi, Appl. Catal. B 30 (2001) 287–292.
[55] A. Hammoudeh, S. Mahmoud, J. Mol. Catal. A 203 (2003) 231–239.
[56] S. Mahmoud, A. Hammoudeh, S. Gharaibeh, J. Melsheimer, J. Mol. Catal. A 178 (2002) 161–167.
[57] G.R. Cairns, R.J. Cross, D. Stirling, J. Catal. 166 (1997) 89–97.
[58] S. Bhogeswararao, D. Srinivas, Catal. Lett. 140 (2010) 55–64.
[59] J. Zhu, Y. Jia, M. Li, M. Lu, J. Zhu, Ind. Eng. Chem. Res. 52 (2013) 1224–1233.
[60] A. Giroir-Fendler, D. Richard, P. Gallezot, Stud. Surf. Sci. Catal. 41 (1988) 171–178.
[61] A. Cabiac, T. Cacciaguerra, P. Trens, R. Durand, G. Delahay, A. Medevielle, D. Plee, B. Coq, Appl. Catal. A 340 (2008) 229–235.
[62] W.M.S. Ide, B. Hao, M. Neurock, R.J. Davis, ACS Catal. 2 (2012) 671–683.
[63] M. Lasdaf, A.O.I. Krause, M. Linbad, M. Tiitta, T. Venalainen, Appl. Catal. A 241 (2003) 65–75.
[64] M.L. Toebes, Y. Zhang, J. Hajek, T.A. Nijhuis, J.H. Bitter, A.J. van Dillen, D.Y. Murzin, D.C. Koningsberger, K.P. de Jong, J. Catal. 226 (2004) 215–225.
[65] Z.-T. Liu, C.-X. Wang, Z.-W. Liu, J. Lu, Appl. Catal. A 344 (2008) 114–123.
[66] Y.-C. Hong, K.-Q. Sun, G.-R. Zhang, R.-Y. Zhong, B.-Q. Xu, Chem. Commun. 47 (2011) 1300–1302.
[67] J.P. Breen, R. Burch, J. Gomez-Lopez, K. Griffin, M. Hayes, Appl. Catal. A 268 (2004) 267–274.
[68] F. Delbecq, P. Sautet, J. Catal. 152 (1995) 217–236.
[69] F. Delbecq, P. Sautet, J. Catal. 211 (2002) 398–406.
[70] E. Bus, J.T. Miller, J.A. van Bakhoven, J. Phys. Chem. B 109 (2005) 14581–14587.
[71] J. Zhao, X. Xu, X. Li, J. Wang, Catal. Commun. 43 (2014) 97–102.
[72] A. Wang, X.Y. Liu, C.-Y. Mou, T. Zhang, J. Catal. (2013), http://dx.doi.org/10.1016/j.jcat.2013.08.023.
[73] V. Ponec, Appl. Catal. A 149 (1997) 27–48.
[74] A. Sarkany, P. Hargittai, A. Horvath, Top. Catal. 46 (2007) 121–128.